

Preparation and Properties of BiFeO₃-PbTiO₃ Thin Films by Chemical Solution Deposition

Asaki Iwata, Tetsuo Shimura, Wataru Sakamoto and Toshinobu Yogo

EcoTopia Science Institute, Nagoya University,

Furo-cho, Chikusa-ku, Nagoya 464-8603, Japan,

Fax : 81-52-789-2133, E-mail : sakamoto@esi.nagoya-u.ac.jp

Ferroelectric (1-x)BiFeO₃-xPbTiO₃ thin films with near the morphotropic phase boundary (MPB) composition have been prepared by the chemical solution deposition. Perovskite BiFeO₃-PbTiO₃ single-phase thin films on Pt/TiO_x/SiO₂/Si substrates with good surface morphology were successfully fabricated by optimizing several processing conditions. Typical polarization (*P*)-electric field (*E*) hysteresis loops were observed for (1-x)BiFeO₃-xPbTiO₃ (x=0.2, 0.3, 0.4) thin films, although some leakage current components were included at room temperature. Since the electrical resistivity of the BiFeO₃-PbTiO₃ films was improved in the low temperature region, those films exhibited well-saturated ferroelectric *P-E* hysteresis loops. The remanent polarization (*P_r*) and coercive field (*E_c*) of the 600°C-prepared 0.7BiFeO₃-0.3PbTiO₃ thin films at -190°C were approximately 60 μC/cm² and 300 kV/cm, respectively.

Key Words: BiFeO₃-PbTiO₃, chemical solution deposition, thin film, ferroelectric properties

1. INTRODUCTION

Recently, BiFeO₃-based thin films have been receiving great attention, because large remanent polarizations more than 50 μC/cm² were reported for BiFeO₃ thin films fabricated by pulsed laser deposition with precise oxygen-partial-pressure control [1-3]. However, in general, the preparation of pure BiFeO₃ without traces of impurities is usually difficult due to the low structural stability of perovskite BiFeO₃ with a relatively low tolerance factor. For thin-film fabrication, the crystallization of the BiFeO₃ phase on substrates often results in the formation of a bismuth-deficient second phase such as Bi₂Fe₄O₉. Bi₂Fe₄O₉ is considered to degrade the surface morphology owing to exaggerated grain growth, leading to poor electrical properties [4]. Therefore, the crystallization of the perovskite BiFeO₃ single phase is indispensable for fabricating thin films having high performance. Moreover, the low resistivity of BiFeO₃ makes the observation of the ferroelectric polarization (*P*)-electric field (*E*) hysteresis loop very

difficult.

Therefore, BiFeO₃-ABO₃ solid solution systems have attracted great attention as a means to improve the structural stability. Among perovskite ABO₃ compounds, PbTiO₃ is a stable ferroelectric perovskite oxide with a Curie temperature of 490°C. A solid solution of BiFeO₃ and PbTiO₃ is expected to achieve the desired structural stabilization and excellent electrical properties. The (1-x)BiFeO₃-xPbTiO₃ system was reported to exhibit high Curie temperatures from ferroelectric to paraelectric phases [5]. Modified BiFeO₃-PbTiO₃ ceramics also have excellent ferroelectric and piezoelectric properties near the morphotropic phase boundary (MPB) composition separating the rhombohedral and tetragonal phases [6]. The MPB of the (1-x)BiFeO₃-xPbTiO₃ system was located around x=0.3 composition according to the literature [5, 7].

In this work, the fabrication and characterization of (1-x)BiFeO₃-xPbTiO₃ (x=0.2, 0.3, 0.4) thin films with near the morphotropic phase boundary (MPB)

composition on Si-based substrates have been performed by chemical solution deposition. The crystallization, surface morphology and ferroelectric properties of chemically derived $\text{BiFeO}_3\text{-PbTiO}_3$ thin films on $\text{Pt/TiO}_x/\text{SiO}_2/\text{Si}$ substrates were examined.

2. EXPERIMENTAL PROCEDURE

$\text{Bi}(\text{O}^i\text{C}_5\text{H}_{11})_3$, $\text{Fe}(\text{OC}_2\text{H}_5)_3$, $\text{Pb}(\text{CH}_3\text{COO})_2$, and $\text{Ti}(\text{O}^i\text{C}_3\text{H}_7)_4$ were selected as starting materials for the preparation of $(1-x)\text{BiFeO}_3\text{-}x\text{PbTiO}_3$ ($x=0.2, 0.3, 0.4$) precursor solutions. The appropriate amounts of $\text{Bi}(\text{O}^i\text{C}_5\text{H}_{11})_3$, $\text{Fe}(\text{OC}_2\text{H}_5)_3$, $\text{Pb}(\text{CH}_3\text{COO})_2$, and $\text{Ti}(\text{O}^i\text{C}_3\text{H}_7)_4$ corresponding to the desired compositions with 3 mol% of excess Bi and 5 mol% of excess Pb were dissolved in absolute 2-methoxyethanol. Then, the mixed solution was refluxed for 20 h yielding a 0.2 M homogeneous precursor solution. The entire procedure was conducted in a dry nitrogen atmosphere.

$\text{BiFeO}_3\text{-PbTiO}_3$ (BF-PT) thin films were fabricated using the precursor solution by spin coating on $\text{Pt/TiO}_x/\text{SiO}_2/\text{Si}$ substrates. As-deposited BF-PT precursor films were dried at 150°C for 5 min and calcined at 400°C at a rate of $10^\circ\text{C}/\text{min}$ for 1 h in an oxygen flow. The calcined films were then crystallized at 600°C at a rate of $10^\circ\text{C}/\text{min}$ for 1 h in an oxygen flow. The thickness of the BF-PT films was adjusted to be approximately 500 nm by repeating the coating / calcining cycle.

The crystallographic phases of prepared BF-PT thin films were characterized by X-ray diffraction (XRD) analysis using $\text{Cu K}\alpha$ radiation with a monochromator. The surface morphology of the crystallized thin films was observed by atomic force microscopy (AFM). The Pt top electrodes with a diameter of 0.2 mm were deposited by DC sputtering onto the surface of the BF-PT films followed by annealing at 400°C for 1 h. The ferroelectric properties of the films were evaluated using a ferroelectric test system (FCE-1, Toyo Corp.) at room temperature. Moreover, the measurement of the ferroelectric properties of the thin films at low temperatures was conducted in a wafer cryostat (Sanwa, WM-363-1) under vacuum (1.0 Pa).

3. RESULTS AND DISCUSSION

3.1 Crystallization of BF-PT thin films on substrates

Fig. 1 shows XRD patterns of $(1-x)\text{BiFeO}_3\text{-}x\text{PbTiO}_3$ (BF-100xPT, $x=0.2, 0.3, 0.4$) thin films fabricated on $\text{Pt/TiO}_x/\text{SiO}_2/\text{Si}$ substrates after heat treatment at 600°C . The BF-20PT, BF-30PT and BF-40PT thin films crystallized in the perovskite BF-PT single phase with random orientations. The crystallization in perovskite BF-PT is due to the stabilization of the perovskite phase by the formation of a solid solution with PbTiO_3 . At a crystallization temperature of 700°C , BF-20PT thin films with a relatively low PbTiO_3 content crystallized in a mixture of perovskite BF-PT and $\text{Bi}_2\text{Fe}_4\text{O}_9$. The formation of $\text{Bi}_2\text{Fe}_4\text{O}_9$ phase is attributed to the low structural stability of perovskite BF-PT and the volatility of Bi and Pb ions at high temperatures. In the BF-PT system, the stability of the perovskite phase is considered to decrease with increasing BiFeO_3 concentration. On the other hand, BF-30PT and BF-40PT thin films crystallized in the single-phase BF-PT at $600\text{-}700^\circ\text{C}$ because no diffraction of the second phase was observed in this composition range.

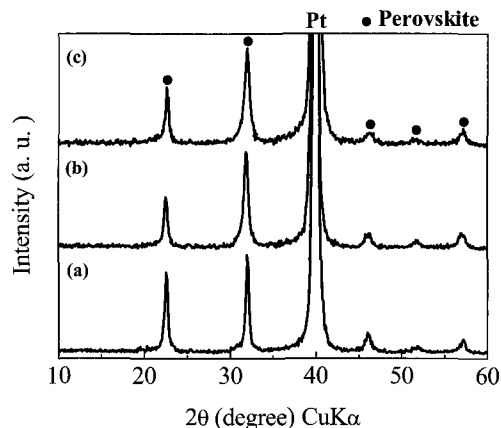


Fig. 1 XRD patterns of $(1-x)\text{BiFeO}_3\text{-}x\text{PbTiO}_3$ (BF-100xPT) thin films on $\text{Pt/TiO}_x/\text{SiO}_2/\text{Si}$ substrates after heat treatment at 600°C (a) BF-20PT, (b) BF-30PT and (c) BF-40PT

3.2 Surface morphology of BF-PT thin films

Fig. 2 shows AFM images of $(1-x)\text{BiFeO}_3\text{-}x\text{PbTiO}_3$ (BF-100xPT, $x=0.2, 0.3, 0.4$) thin films prepared at 600°C on $\text{Pt/TiO}_x/\text{SiO}_2/\text{Si}$ substrates. It revealed from Fig. 2 that the surface morphology of the BF-PT thin films slightly depended on the PbTiO_3 content in this

composition range. The root-mean-square (RMS) roughness values of the BF-20PT, BF-30PT and BF-40PT thin films were 3.7, 3.1, and 3.4 nm, respectively. On the contrary, the average grain size of the BF-PT thin films varied as shown in Fig. 2, and was affected by the amount of PbTiO₃. In addition, with increasing crystallization temperature, the surface morphology of the BF-PT thin films degraded. In particular, BF-20PT thin films crystallized at higher temperatures had larger RMS roughness. This may be due to the exaggerated grain growth through the formation of the second phase (Bi₂Fe₄O₉, etc.) accompanied by the volatilization of Bi and Pb ions. On the other hand, the RMS roughness of the perovskite BF-30PT and BF-40PT thin films did not largely depend on the crystallization temperature.

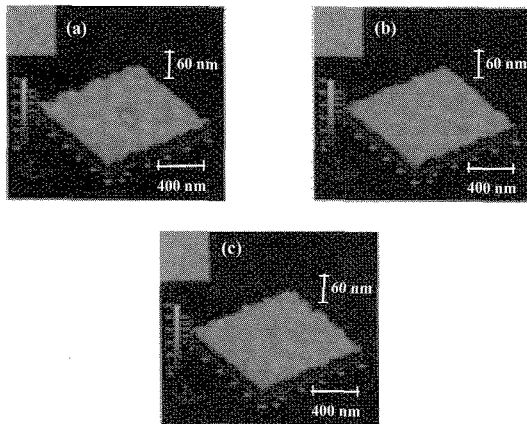


Fig. 2 AFM images of $(1-x)\text{BiFeO}_3-x\text{PbTiO}_3$ (BF-100xPT) thin films on Pt/TiO_x/SiO₂/Si substrate after heat treatment at 600°C (a) BF-20PT, (b) BF-30PT and (c) BF-40PT

3.3 Ferroelectric properties of BF-PT thin films

P - E hysteresis measurements were also performed to characterize the ferroelectricity for $(1-x)\text{BiFeO}_3-x\text{PbTiO}_3$ (BF-100xPT, $x=0.2, 0.3, 0.4$) thin films crystallized at 600°C. Fig. 3 shows the P - E hysteresis loops of $(1-x)\text{BiFeO}_3-x\text{PbTiO}_3$ (BF-100xPT, $x=0.2, 0.3, 0.4$) thin films measured at room temperature. Although these thin films showed ferroelectric hysteresis loops, the shape of the P - E curves is not good because of the lack of electrical resistivity in the synthesized thin films. One of the major problems of BiFeO₃-based thin films is their low electrical resistivity, which affects the measurement

of ferroelectric properties at room temperature. This is derived mainly from the valence fluctuation of Fe³⁺ to Fe²⁺ generating oxygen vacancies for charge compensation. The hopping electrons between Fe³⁺ and Fe²⁺ in BF-PT degrade the insulation resistance of resultant thin films.

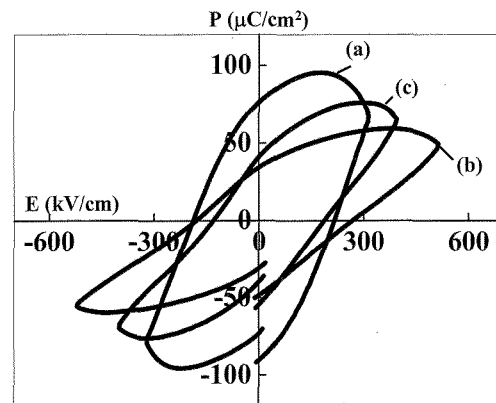


Fig. 3 P - E hysteresis loops of 500-nm-thick $(1-x)\text{BiFeO}_3-x\text{PbTiO}_3$ (BF-100xPT) thin films after heat treatment at 600°C measured at room temp. (a) BF-20PT, (b) BF-30PT and (c) BF-40PT

Measurement at low temperature was then performed, since the electrical resistivity was supposed to be high enough to characterize net ferroelectricity of the synthesized thin films. Fig. 4 shows P - E hysteresis loops of $(1-x)\text{BiFeO}_3-x\text{PbTiO}_3$ (BF-100xPT, $x=0.2, 0.3, 0.4$) thin films measured at -190°C. These thin films showed relatively well-saturated ferroelectric hysteresis loops compared with those at room temperature shown in Fig. 3. Among these films, BF-30PT thin films showed the largest ferroelectricity. The remnant polarization (P_r) and coercive field (E_c) of the 600°C-prepared BF-30PT thin films were approximately 60 $\mu\text{C}/\text{cm}^2$ and 300 kV/cm^2 , respectively. The 600°C-prepared BF-20PT and BF-40PT thin films exhibited smaller P_r values around 40 $\mu\text{C}/\text{cm}^2$. These P_r values were higher than those reported for La- and Ga-modified BF-PT bulk ceramics with compositions near the MPB [6]. However, the E_c values of the BF-PT films were inferior to those of BF-PT-based ceramics. To realize a practical application of the BF-PT thin films, the improvement of ferroelectric properties at ambient temperature is strongly required and it is currently under investigation.

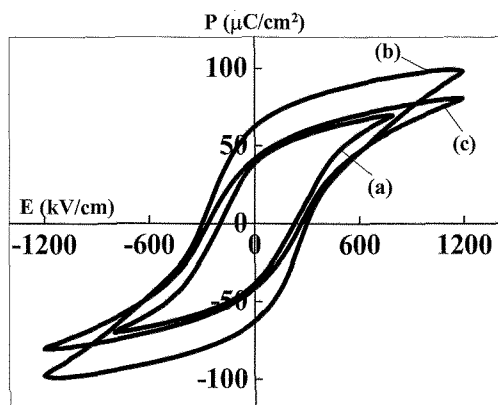


Fig. 4 P - E hysteresis loops of 500-nm-thick $(1-x)\text{BiFeO}_3\text{-}x\text{PbTiO}_3$ (BF-100 x PT) thin films after heat treatment at 600°C measured at -190°C (a) BF-20PT, (b) BF-30PT and (c) BF-40PT

4. CONCLUSIONS

Ferroelectric $(1-x)\text{BiFeO}_3\text{-}x\text{PbTiO}_3$ (BF-100 x PT, $x=0.2, 0.3, 0.4$) thin films were successfully synthesized by the chemical solution deposition. Perovskite $\text{BiFeO}_3\text{-PbTiO}_3$ single-phase thin films with a RMS roughness value less than 4 nm could be fabricated by optimizing the several processing conditions. Although the electrical resistivity was not sufficiently high around room temperature, the potential ferroelectricity of the synthesized films was revealed at low temperatures. The BF-30PT thin films were found to exhibit the P_r value of $60 \mu\text{C}/\text{cm}^2$ at -190°C .

REFERENCES

- [1] J. Wang, J. B. Neaton, H. Zheng, V. Nagarajan, S. B. Ogale, B. Liu, D. Viehland, V. Vaithyanathan, D. G. Schlom, U. V. Waghmare, N. A. Spaldin, K. M. Rabe, M. Wuttig and R. Ramesh, *Science*, **299**, 1719 (2003).
- [2] K. Y. Yun, D. Ricinschi, T. Kanashima, M. Noda and M. Okuyama, *Jpn. J. Appl. Phys.*, **43**, L647 (2004).
- [3] F. Bai, J. Wang, M. Wittig, J.-F. Li, N. Wang, A. P. Pyatakov, A. K. Zvezdin, L. E. Cross and D. Viehland, *Appl. Phys. Lett.*, **86**, 032511 (2005).
- [4] F. Tyholdt, S. Jorgensen, H. Fjellvag and A. E. Gunnaes, *J. Mater. Res.*, **20**, 2127 (2005).
- [5] S. A. Fedulov, P. B. Ladyzhinskii, I. L. Pyatigorskaya and Y. N. Venevtsev, *Sov. Phys. Solid State*, **6**, 375 (1964).

[6] J.-R. Cheng and L. E. Cross, *J. Appl. Phys.*, **94**, 5188 (2003).

[7] D. I. Woodward, I. M. Reaney, R. E. Eitel and C. A. Randall, *J. Appl. Phys.*, **94**, 3313 (2003).

(Received December 15, 2006; Accepted December 22, 2006)